Accepted Manuscript

Title: A comparison of the genotoxicity of benzo[*a*]pyrene in four cell lines with differing metabolic capacity

Author: Ume-Kulsoom Shah Anna L Seager Paul Fowler Shareen H Doak George E Johnson Sharon J Scott Andrew D Scott Gareth JS Jenkins

PII: S1383-5718(16)30016-X
DOI: http://dx.doi.org/doi:10.1016/j.mrgentox.2016.06.009
Reference: MUTGEN 402760

To appear in: *Mutation Research*

Received date: 16-1-2016
Revised date: 3-6-2016
Accepted date: 6-6-2016

Please cite this article as: Ume-Kulsoom Shah, Anna L Seager, Paul Fowler, Shareen H Doak, George E Johnson, Sharon J Scott, Andrew D Scott, Gareth JS Jenkins, A comparison of the genotoxicity of benzo[a]pyrene in four cell lines with differing metabolic capacity, Mutation Research/Genetic Toxicology and Environmental Mutagenesis http://dx.doi.org/10.1016/j.mrgentox.2016.06.009

A comparison of the genotoxicity of benzo[*a*]pyrene in four cell lines with differing metabolic capacity

Ume-Kulsoom Shah[1], Anna L Seager[1], Paul Fowler[2], Shareen H Doak[1], George E Johnson[1], Sharon J Scott[2], Andrew D Scott[2], Gareth J S Jenkins[1]*

[1]Institute of Life Sciences, College of Medicine, Swansea University, Singleton Park, Swansea SA2 8PP.

[2]Safety & Environmental Assurance Centre (SEAC), Unilever, Bedford, MK44 1LQ, UK

*To whom correspondence should be addressed. Tel: +44 179 260 2512; Email: G.J.Jenkins@swansea.ac.uk

A comparison of the genotoxicity of benzo[*a*]pyrene in four cell lines with differing metabolic capacity

Highlights

- *In vitro* metabolic efficiency of Benzo[*a*]pyrene
- MCL-5 and HepG2 cell lines gave significant genotoxiity after 4h and 24h treatments
- CYP450 enzymes and m*EH* in gentotoxicity and mutagenicity

ABSTRACT

Benzo[*a*]pyrene (B[*a*]P) is a known genotoxin and carcinogen, yet its genotoxic response at low level exposure has not been determined. This study was conducted to examine the interplay of dose and metabolic capacity on genotoxicity of B[*a*]P . Investigating and better understanding the biological significance of low level chemical exposures will help improve human health risk assessments. The genotoxic and mutagenic effects of B[*a*]P were investigated using human cell lines (AHH-1, MCL-5, TK6 and HepG2) with differential expression of the CYP450 enzymes (CYP1A1, 1B1 and1A2 involved in B[*a*]P metabolism. MCL-5 and HepG2 cells showed detectable basal expression and activity of CYP1A1, 1B1 and 1A2 than AHH-1 which only show CYP1A1 basal expression and activity. TK6 cells showed negligible expression levels of all three CYP450 enzymes. *In vitro* micronucleus and HPRT assays were conducted to determine the effect of B[*a*]P on chromosome damage and point mutation induction. After 24h exposure, linear increases in micronucleus (MN) frequency were observed in all cell lines except TK6. After 4h exposure, only the metabolically competent cell lines MCL-5 and HepG2 showed MN induction (with a threshold concentration at 25.5µM from MCL-5 cells) indicating the importance of exposure time for genotoxicity. The HPRT assay also displayed linear increases in mutant frequency in MCL-5 cells, after 4h and 24h treatments. Mutation spectra analysis of MCL-5 and AHH-1 HPRT mutants revealed frequent B[*a*]P induced G to T transversion mutations (72% and 44% of induced mutations in MCL-5 and AHH-1 respectively). This study therefore demonstrates a key link between metabolic capability, B[*a*]P exposure time and genotoxicity.

Key words: Genotoxicity; Mutagenicity; Dose-response; Metabolic activation; Threshold; Micronucleus assay; HPRT assay

1. Introduction

Genotoxins are chemicals that induce DNA mutations that can lead to cancer. Mutation in genes essential to perform normal regulatory processes like controlled cell signalling, cell cycle checkpoints and apoptosis, can lead to cancer development [1]. Some genotoxic chemicals, when released into the environment, can remain intact for long periods of time and cause adverse effects. It is important to assess the genotoxic potential of such chemicals for a better understanding of their carcinogenicity in order to reduce the potential risk of human cancer and other diseases involving acquired mutations in the somatic cells.

The link between environmental chemical exposure and human disease was first recorded in 1775 with the discovery of chimney sweeper's cancer (soot wart), a squamous cell carcinoma of the skin of the scrotum, which originated from the components of soot [2]. The first report of the induction of squamous cell papilloma on rabbit ears after repeated exposure of coal tar, was published in 1918 [3]. Kennaway, in 1930, found that tumours in mouse skin could be produced by pure 1, 2, 5, 6 dibenzanthracene [4]. Later on in 1932, Cook and colleagues successfully isolated polycyclic aromatic hydrocarbon, benzo[*a*]pyrene (PAH, B[*a*]P) from coal tar, a highly carcinogenic crystalline compound [5].

B[*a*]P belongs to a family of chemicals that can act like dioxins, based on a common mechanism of toxic action. Like dioxin compounds, PAHs have biologic responses mediated via binding to the aryl hydrocarbon receptor (AhR) which is a specific high-affinity cellular reporter protein [6] despite PAHs being quite different structurally from dioxins. Due to their potential risk to humans and animals, the United States Environmental Protection Agency (US-EPA) has designated 126 PAHs as priorities for environmental concern and B[*a*]P is one which is frequently monitored in the environment. B[*a*]P is generated through the burning of fossils fuels or wood, vehicle exhaust emission, heat and power generation, industrial processes or oil contamination and is always found environmentally as a mixture with other PAHs as in cigarette smoke, charcoal-cooked food and industrial waste by-products [7, 8].

Human environmental exposure to B[*a*]P mainly occurs through cigarette smoking and the ingestion of contaminated food and water [7], with significant concentrations found in Western diet such as in fried and grilled meats. Both environmental and dietary factors are associated with an increased risk of different organ cancers [9], autoimmune [10] and inflammatory diseases [11]. The daily intake of B[*a*]P in the average human

diet has been estimated to range from 120- 2800ng/day [12] and concentration of B[*a*]P in full flavoured cigarettes has also been reported to be about 10ng per cigarette [13, 14], which is equivalent to an intake of about 200ng/day for a pack-a-day cigarette smoker [15]. B[*a*]P is transported across the cell membrane by lipoproteins [16] and B[*a*]P's presence activates the Aryl hydrocarbon receptor (AhR), which in turn binds with AhR nuclear translocator (ARNT) and induces the expression of genes involved in B[*a*]P metabolism as well as other genes that are not related to B[*a*]P metabolism. Several other genes such as the cytochrome P450 genes *CYP1A1*, *CYP1A2*, and *CYP1B1*, and glutathione-S-transferase (*GST*) and UDP-glucuronosyltransferase (*UGT-1*) are also induced via AhR-mediated pathways. Indeed, the relative expression of phase I and phase II enzymes determines the ratio of activation and detoxification of B[*a*]P. B[*a*]P is often first oxidized at the bay region by phase I *CYP1A1* into B[*a*]P-7,8-epoxide, which through hydration by microsomal epoxide hydrolase (*mEH*) is metabolized to B[*a*]P-7,8-dihydrodiol (BPD). BPD serves as a substrate for a second CYP dependent oxidation reaction and generates the metabolite B[*a*]P-7,8-dihydrodiol-9,10-epoxide (BPDE) [17]. BPDE contains an epoxide ring within the bay region making it highly reactive with DNA in a time dependent manner.

The genotoxicity of most direct acting genotoxins is dependent on the dose and length of exposure whereby genotoxic effects are observed at or above a critical dose. These doses are referred to as threshold doses, below which no observable genotoxic effect is seen. Nowadays a threshold level is commonly used to determine or establish a safe limit of a chemical for human use but only when their mechanism of action is established and accepted by risk assessment agencies. This threshold limit is derived from a combination of dose-dependent responses, mathematical and statistical models, to cover any variability, and risk assessment procedures. Typically a threshold level is a value between a no observable effect level (NOEL) and lowest observable effect level (LOEL) [18] and can be confirmed by mathematical modelling [19]. The nature of the chemical, its interaction with the non-DNA targets, and cell protective mechanisms (detoxification, DNA repair, etc.) are the mechanistic factors that influence dose-dependent responses [19]. Therefore, it is important to consider these factors while assessing if thresholds exist for any genotoxins. These considerations become even more complex if the genotoxin involved is a pro-carcinogen that requires metabolic activation to initiate

genotoxicity. As compared to direct acting agents, little is known about the threshold doses of pro-carcinogenic agents and the critical factors controlling dose response relationships for genotoxicity.

Considering this, the aim of this study was to identify the dose responses at the low dose range of B[*a*]P and determine whether there is differential genotoxicity and mutagenicity of B[*a*]P in different human cell lines based on their metabolic capacity of phase I enzymes. The cell lines used in the present study were human lymphoblastoid cell lines AHH-1, MCL-5, TK6 and primary hepatoblastoma cell line HepG2, known to have differential expression of phase I CYP450 enzymes. AHH-1 cell line only expresses CYP1A1, MCL-5 cells express all five CYP450 enzymes (detailed information for each cell line in Material and Method section). TK6 cells were used as a control as they are devoid of CYP450 enzymes. Therefore, all of these cell lines serve as a good tool to investigate the role of P450 enzymes in assessing the genotoxicity of chemicals that require metabolic activation. The stable expression system also furthers understanding of the process from metabolic activation of test compounds to the appearance of toxicological consequences entirely in the same intact cells. The study utilised the *in vitro* cytokinesis blocked micronucleus (CBMN) assay and hypoxanthine (guanine) phosphoribosyltransferase (H(G)PRT) assay in human cell lines to examine the induction of chromosomal damage and the frequency and spectra of point mutations, respectively. CYP450 enzymes levels and activity were also investigated in parallel through gene expression analysis and reporter assays.

2. Materials and Methods

2.1 Reagents

HAT supplement (2×10^{-4}M hypoxanthine, 8×10^{-7}M aminopterin, and 3.5×10^{-5}M thymidine), HT supplement (2×10^{-4}M hypoxanthine and 3.5×10^{-5}M thymidine) were purchased from Invitrogen (Paisley, UK), 6-thioguanine, B[*a*]P, trypsin, hygromycin B, dimethyl sulfoxide (DMSO) and phosphate buffered saline (PBS) were purchased from Sigma (Gillingham, UK). N-Cyclohexyl-*N*-dodecylurea (NCND) was purchased from Calbiochem (EMD Chemicals Inc. US). Cytochalasin B was from Merck (Darmstadt, Germany). All powdered reagents were reconstituted according to manufacturer's instructions. All chemical dilutions were freshly prepared from stock solutions and for each experiment new stock was prepared.

2.2 Cell Culture

The present study utilised human male lymphoblastoid cell lines AHH-1, MCL-5 (ATCC, Middlesex, UK), TK6 and human hepatoma cell line HepG2 (ECACC, Salisbury, UK). The cell cycle doubling time for TK6 was 18h, for AHH-1 and MCL-5 22-24h, and 26-28h for HepG2. TK6 was isolated from WIL2, heterozygous at thymidine kinase (TK) locus and has a stable and wild-type *p53* gene but minimal or no expression of CYP450 enzymes.

AHH-1 is a TK+/- with native CYP1A1 activity which was used for oxidative xenobiotic metabolism and was devoid of microsomal epoxide hydrolase [20]. It has +/- *p53* gene.

MCL-5 cell line was a derivative of AHH-1 TK+/- that has been transfected with 4 cDNAs of the human CYP450s (carried on plasmids). These cDNAs include *CYPA12, CYP2A6, CYP3A4* and *CYP2E1* and microsomal epoxide hydrolase (*mEH*). MCL-5 has been shown to be more sensitive than AHH-1 TK+/- to the mutagenic properties of many pro-mutagens and pro-carcinogens and direct acting agents [21]. The plasmids were maintained in these cells through hygromycin (B) resistant genes. Both AHH-1 and MCL-5 harbour a heterozygous transition (C>T) p53 mutation at the codon 281/282 interface within exon 8, it retains the ability to undergo DNA damage–induced apoptosis and has been reported to express *p53* which can be phosphorylated [22].

HepG2 cells were isolated by Aden *et a*l, (1997) from a primary hepatoblastome of an 11-year-old Argentine boy [23]. HepG2 have epithelial like morphology which resembles liver parenchymal cells and retain many of the specialized functions in culture such as secretion of major plasma proteins [24]. This cell line is a useful model of human liver cells and expresses many functional phase I and phase II xenobiotic metabolic enzymes [25].

All media used were purchased from GIBCO® (Life technologies, Paisley, UK) unless otherwise stated. The cell lines AHH-1, MCL-5, and TK6 were cultured in RPMI 1640 supplemented with 1% L-glutamine and 10% donor horse serum (BD Gentest, Oxford, UK) in 80-cm^2 flasks at 37°C, 5% CO_2. In addition, MCL-5 cells were supplemented with hygromycin B at each passage to ensure plasmid retention. The cells were maintained at a concentration of 1-2 x 10^5 cells/ml. HepG2 cell line was cultured in DMEM, supplemented with 10% foetal bovine serum and Pen/strep (penicilin and streptomycin [10,000U/ml]) and maintained at a concentration of

1.5-2 x 10^5 cells/cm^2. Each experiment was repeated three times and each replicate was independently produced on different days.

2.3 Treatment with B[a]P

For the CBMN assay all cell lines were treated with B[*a*]P for 4h or 24h followed by one cell cycle of cytochalasin B (3-6µg/ml depending on the cell type being used). The treatment regimes chosen (1-70µM) covered a range of doses, with the top concentration chosen as it produced less than 55+/-5% cytotoxicity, and thus any observed chromosome damage induction could not be contributed as a secondary effect of cytotoxicity [26]. For the HPRT assay, AHH-1 and MCL-5 cells were treated with B[*a*]P for 24h with 1, 2, 3, 4, 5 and 10µM B[*a*]P. In 4h B[*a*]P treatment these cell lines were treated with 5, 10, 15, 20, 25, 30 and 50µM B[*a*]P. The highest concentration of B[*a*]P used here caused a maximum of 40+/-5% toxicity as adjusted by plating efficiency (PE). This is within the acceptable range for testing as described in the OECD guidelines 476 [27]. For the measurement of *CYP1A1*, *CYP1B1*, and *CYP1A2* expressions and activities all cell lines were treated with LOELconcentration and concentration above LOEL of B[*a*]P for 24h, obtained as a result of CBMN assay. All the washing steps involved were done at room temperature and all centrifugation steps performed at (300 x g) for 5min.

2.4 Cytotoxicity assessment using relative population doubling

The cytotoxicity of B[*a*]P dissolved in DMSO was determined by relative population doubling (RPD) in the absence of cytochalasin B following the procedure described by Brüsehafer *et al*. [28] with a few modifications. HepG2 cells were seeded at 1.2x10^5 cells/cm^2 at 37ºC, 5% CO_2, cells from each treatment flask were counted (control treatment) with the Beckman coulter counter (Z1 Coulter Particle Counter, Beckman, UK) and incubated for 24h. AHH-1, MCL-5 and TK6 cells were seeded at 1x10^5 cells/ml for 24h and cells were counted (control treatment) from each flask 1h before treatment. All four cell lines were again counted at the cell harvest stage (treated cultures).

2.5 The Cytokinesis blocked micronucleus assay

Micronuclei (MN) frequency was utilized to assess the *in vitro* level of chromosomal damage induction. The assay was performed as previously described by Seager *et al.* [29] with a few modifications. AHH-1, MCL-5 and TK6 (10ml) suspensions of cells at 1 x 10^5 cells/ml and HepG2 at 1.2 x 10^5 cells/cm^2, were seeded for 24h at 37°C, 5% CO_2. Flasks were treated with appropriately diluted B[*a*]P for 4h or 24h, after which AHH-1, MCL-5 and TK6 cells were centrifuged (pipetted off the medium from HepG2 flasks), washed twice with RPMI 1640 (without supplement), and re-suspended in 10ml fresh media containing 6µg/ml cytochalasin B for one cell cycle (22h for AHH-1 and MCL-5 and 26h for HepG2), 3µg/ml for TK6 (18h). Treated cells (AHH-1, MCL-5 and TK6) were washed twice by centrifugation with PBS while HepG2 cells were washed twice and then trypsinised. Slides were prepared for the Metafer 4 software, version 3.8.5 (MetaSystems, Altlussheim, Germany) as described by Seager *et al.* [30]. A minimum of 3333 binucleated cells were scored per replicate, and each treatment was performed in triplicate (an average of 10,000 binucleates per treatment).

2.6 The hypoxanthine phosphoribosyltransferase assay

The *in vitro* HPRT assay was used to study the gene mutations at *HPRT* locus.To reduce the background mutants, AHH-1 and MCL-5 cells were cultured for 3 days in RPMI 1640 containing 50X HAT media, which is lethal to cells that harbour mutations at the HPRT. Subsequently, the cells were transferred to media containing 50X HT media for 24h and then grown in normal media for two days to achieve sufficient cell number for treatments.

The assay was performed as previously described by Doak *et al*. [31], with the following modifications: AHH-1and MCL-5 cell suspensions (10 ml), at 4 x 10^5 cells/ml, were exposed to the test chemical in 80-cm^3 flasks at the appropriate concentration for 4h or 24h at 37°C, 5% CO_2. It was noted by using the two-tailed *t*-test that the mutant frequency (MF) of the solvent control (DMSO) is non-significantly different from that of the untreated control, with MF being 0.18×10^{-5} ± 0.03 (mean ± SE) and 0.26×10^{-5} ± 0.03, respectively for AHH-1 and 2.2×10^{-5} ± 0.15 (mean ± SE) and 2.39×10^{-5} ± 0.13, respectively for MCL-5.

2.7 Clonal expansion of mutants

Solvent control and 10µM B[*a*]P treated HPRT mutant colonies were transferred to 24-well plates containing 2ml growth medium per well and grown for 5 days at 37°C, 5% CO_2, after which 300µl of the individual colony was carefully extracted and mixed with 1.5 ml RNA protect (1:5, Sigma, UK) and stored at -20°C for RNA extraction.

2.8 RNA extraction and cDNA amplification

Total cellular RNA was extracted using the RNeasy mini kit (Qiagen, West Sussex, UK) with DNase treatment and RETROscript® kit (Ambion, Sussex, UK) was used for cDNA synthesis, according to the manufacturer's instructions. End-point PCR of cDNA was performed by using a GoTaq® Flexi DNA Polymerase kit (Promega, Southampton, UK), on an iCycler (Bio-Rad, Hemel Hemstead, UK). The β-actin primers (forward: 5′-GATGGCCACGGCTGCTTC-3′, reverse: 5′- TGCCTCAGGGCAGCGGAA-3′ with product size 100bp) which clarify the cDNA reaction were synthesized by MWG Eurofins (Germany). The HPRT primers used to amplify the HPRT cDNA were previously mentioned by [32]. Separate reactions were established for each primer pair. Approximately 1µg RNA was used for cDNA synthesis and PCR in a reaction volume of 50µl, containing 10µl of 5x colorless GoTaq® Flexi Buffer, 4µl $MgCl_2$ solution, 1µl of dNTP mix, 1µl GoTaq® DNA polymerase, and 1µl of each primer at a final concentration of 0.2µM and 30.7µl of Nuclease-free water. The following PCR reaction protocol was used: initially cDNA production occurred for one cycle at 44°C for 60min followed by 90°C for 10min. Subsequently, PCR was initiated for 31 cycles of 93°C for 2min, 93ºC for 10s, 52.6ºC for 20s, 72ºC for 10s and prior to storage at 4ºC until downstream analysis occurred. Reactions were performed in triplicate, and PCR products were visualized using DNA polyacrylamide gel electrophoresis on 6% polyacrylamide gel followed by 0.1% silver nitrate staining.

2.9 Sample preparation for sequencing

PCR products were purified by using Qiagen PCR purification kit® (Sussex, UK) according to the manufacturer's instructions. Finally, 20µl of each sample was sent to Genome enterprise Limited for forward

and reverse sequencing. Mutations were identified using Mutation Surveyor version 3.0 (Soft genetics, State College, PA). Any mutation found was confirmed by repeat processing.

2.10 Construction of mutation spectra

Mutation spectra were constructed using iMARS sofware [33].

2.11 Expression of CYP450 enzymes using quantitative real-time PCR

The expression of *CYP1A1*, *CYP1B1*, and *CYP1A2* mRNA in human cell lines AHH-1, MCL-5, TK6 and HepG2 was evaluated qualitatively using real-time reverse transcriptase-PCR. MCL-5, AHH-1 and TK6 cells were seeded at a density of $1x10^5$ cells/ml and HepG2 at $1.2x10^5$ cells/cm^2. After 24h incubation cells were exposed for 24h with B[*a*]P. Following the exposure period cells were washed twice and the RNA was extracted as mentioned previously. The purified RNA samples were reverse transcribed using the QuantiTect® Reverse Transcription Kit from Qiagen (Sussex, UK) according to manufacturer's instructions. All the primers were synthesized by Sigma-Aldrich (UK) and the oligonucleotide sequence and product size for each primer were as follows; *CYP1A1*- forward, 5′-ATCCTTGTGATCCCAGGCTCC-3′, reverse, 5′-TAGGGATCTTGGAGGTGGCTGA-3′ with product size 76bp, *CYP1A2*- forward, 5′-CCAACGTCATTGGTGCCATG-3′, reverse, 5′-GTGATGTCCCGGACACTGTTC-3′ with product size 262bp and *CYP1B1*-forward,5′-TCCTCCTCTTCACCAGGTATCC-3′, reverse, 5′- TGGTCACCCATACAAGGCAG-3′ with product size 97bp. Real-time PCR was then performed on an iCycler iQ5 Thermal Cycler (Bio-Rad, Hertfordshire, UK) using the QuantiFast SYBR Green PCR Kit (Qiagen). The resultant data were analysed by the standard curve method and genes of interest were normalized against *β-actin*.

2.12 Measurement of CYP450 activity

The CYP450 activity was determined using the P450-Glo 1A1 assay, 1B1 assay and 1A2 assay kits (Promega, USA), according to the manufacturer's instructions. MCL-5, AHH-1 and TK6 cells were seeded at a density of $1x10^5$ cells/ml and HepG2 at $1.2x10^5$ cells/cm^2. After 24h incubation cells were exposed for 24h with

B[*a*]P and washed twice with PBS. For the measurement of CYP1A1 and 1B1, the cells were maintained at $5x10^5$ cells/ml concentration in culture medium. Medium (50µl) containing 5mM luminogenic CYP1A1-CEE was added in 50µl cell suspension in 96 well-plate and incubated at 37°C for 3h. CYP1A2 activity was measured by adding the 50µl diluted Luciferin-1A2 in PBS containing 3mM salicylamide to inhibit the phase II conjugation of the CYP product from CYP1A2-Luciferin 1A2, into 50µl cell suspension and incubated for 30min. Luceferin detection reagent with D-cystene was reconstituted as directed by instructions for use. An equal volume of Luciferin Detection Reagents were added at the end of the incubation period to the cells to measure the activity after 10min on FLOURstar OPTIMA (BMG Lab technologies Ltd., UK). CYP450 activities were calculated by subtracting the background and normalizing to the seeded cell number.

2.13 Statistical analysis

For the cytotoxicity data error bars, are represented as standard errors (SEs) of the mean. For genotoxicity data a one-way ANOVA approach, followed by two-tailed Dunnett's *post hoc* test, was used to determine if any of the treatment doses were significantly different from the zero dose ($p<0.05$), except in the HPRT assay the control and solvent control were analysed using *t*-test. The hockey stick modelling of apparent thresholds was carried out using software, kindly provided by Lutz and Lutz [34] and implemented in the R package. A one-way ANOVA approach, followed by two-tailed Dunnett's *post hoc* test, was used to determine the basal and induced expression of CYP450 enzymes after B[*a*]P treatments.

3. Results

The present study explored the contribution of metabolic capacity on the genotoxic dose responses obtained for B[*a*]P. The cell lines selected to assess the induction of MN and HPRT mutations by B[*a*]P have varying metabolic competency.

3.1 The CBMN assay to determine B[a]P induced genotoxicity

The cell lines TK6, AHH-1, MCL-5 and HepG2 were tested for their ability to metabolise B[*a*]P into toxic/genotoxic metabolites after 24h exposure, as measured by cell viability and induced DNA damage. B[*a*]P

did not show any significant cytotoxic or genotoxic effects in the TK6 cell line at any of the doses tested 1-70µM (Figure 1A). In contrast to TK6, AHH-1 cells showed a slight increase in cytotoxicity, (55±5% cytotoxicity was not achieved even at highest concentration of 70µM. However, a gradual increase in genotoxic dose response was observed in AHH-1 cells and the frequency of MN (%MN/BN) was significantly increased at a B[*a*]P concentration of 4µM ($p<0.01$) which was the LOEL concentration (Figure 1B). In comparison, the more metabolically competent cell lines showed a greater sensitivity to B[*a*]P with >55% cytotoxicity observed in MCL-5 and HepG2 cells at 25µM and 5µM concentrations respectively (Figures 1C and 1D). Due to the higher cytotoxicity of B[*a*]P in HepG2 cells, studies were restricted to a maximum concentration of 10µM of B[*a*]P. Increases in DNA damage levels (%MN/BN) were observed in both MCL-5 and HepG2 cells after 24h B[*a*]P treatment. The LOEL concentration was 3µM ($p<0.05$) for both cell lines as illustrated in Figure 1C, 1D. The Hockey-stick model analysis revealed a linear dose-response for MN induction after B[*a*]P in AHH-1, MCL-5 and HepG2 cell lines.

In order to explore the effect of a shorter exposure time on B[*a*]P's genotoxicity a 4h exposure CBMN assay was also performed. AHH-1, MCL-5 and HepG2 cells were treated with B[*a*]P using a dose range of 10-70µM for 4h. TK6 was omitted as negative results were seen at 24h. Similar to the 24h B[*a*]P treatment, AHH-1 cells had low cytotoxicity (<55% at the highest concentration of 70µM B[*a*]P), but significant cytotoxicity (>55%) was observed in both MCL-5 and HepG2 cells at 60µM and 10µM B[*a*]P, respectively (Figure 2). In contrast to 24h exposure, no elevation in MN frequency was observed in AHH-1 following B[*a*]P treatment (Figure 2A). A LOEL for MN was observed in MCL-5 cells at 40µM ($p<0.05$) B[*a*]P (Figure 2B), compared to 3µM with 24h exposure above. An increasing genotoxic response was also observed in HepG2 cells with a significant increase in the frequency of MN/BN cells (a LOEL) observed at 20µM ($p<0.05$), compared to 3µM with 24h exposure above. Hockey-stick statistical modelling rejected the linear dose-response and supported the threshold model in MCL-5 cells after 4h exposure and confirmed an estimated inflection point (IP) at 25.46µM ($p<0.002$) with lower confidence interval (CI) of 14.60µM with B[*a*]P. The dose response curve for B[*a*]P in HepG2 cell line was however linear.

3.2 Role of microsomal epoxide hydrolase in micronuclei induction

To confirm the importance of m*EH* in inducing an increased genotoxic potential and potency of B[*a*]P, as shown in MCL-5 cells specifically, N-Cyclohexyl-*N*'-dodecylurea (NCND), an effective inhibitor for m*EH* [37] was used. When MCL-5 cells were pre-treated for 2h with NCND (dose 170nM) and then exposed to 70µM B[*a*]P for 24h MN induction decreased (1.6-fold) and cytotoxicity reduced from 84% to 25% as compared to cells without pre-treatment.

3.3 Mutation frequency at HPRT loci for B[*a*]*P*

The HPRT assay was also performed in both AHH-1 and MCL-5 cells in order to study the mutagenic effect of 4h and 24h exposure of B[*a*]P. The B[*a*]P concentrations selected for this study were low concentrations including the LOEL dose that produced the first significant increase in the CBMN assay. TK6 cells were not used because they did not show any genotoxicity with B[*a*]P, while HepG2 cells are less amenable to the HPRT assay. The AHH-1 cell viability did not vary significantly after treatment with B[*a*]P and the background mutation frequency (MF) of AHH-1 cells was found to be 0.18 $x10^{-5}$ HPRT mutants. Despite low toxicity levels, AHH-1 cells showed increased MF with increasing B[*a*]P concentration (with 24h exposure). MF was significantly increased from 0.18 $x10^{-5}$ in control to 3.14 $x10^{-5}$ at 4µM ($p<0.05$) and 5.52 $x10^{-5}$ at the top concentration of 10µM ($p<0.001$) (Figure 4A). The LOEL detected was 4µM which corresponded with the CBMN assay.

A small reduction in cell viability was observed in MCL-5 cells treated with 3µM B[*a*]P for 24h, yet cell viability was still 74.65% (approximately 25% toxicity) at the top concentration of 10µM. A linear increase in MF was observed over the 1-5µM concentration range, which was followed by a sharp increase in MF at the 10µM concentration. MF was significantly increased from 2.20 $x10^{-5}$ in untreated control cells to 22.96 $x10^{-5}$ at 2µM ($p<0.01$) and 99.3 x 10^{-5} at the highest cencentration of 10µM ($p<0.001$). The LOEL observed was 2µM (less than that of the corresponding MN assay) (Figure 4A). MCL-5 was observed to be far more sensitive than AHH-1 in term of mutation induction. Hockey stick modelling revealed that B[*a*]P exhibited a linear dose-response in both AHH-1 and MCL-5 cells after 24h exposure and no threshold dose was found.

There was a non-significant difference in % cell viability observed in both MCL-5 and AHH-1 cell lines when exposed to B[*a*]P for a shorter time of 4h. The MF was not increased in AHH-1 cells at all but it was significantly elevated with increasing concentration in MCL-5 cell line and the LOEL was found to be 10μM ($p<0.01$) with a linear dose response (Figure 4B), compared to a LOEL at 2μM with 24h exposure.

3.4 Spontaneous and B[a]P-induced Mutations in AHH-1 and MCL-5 HPRT mutants

A clear difference was seen in the patterns of the HPRT mutations from AHH-1 (Table I, Supplementary Table S1A) and MCL-5 (Table I, Supplementary Table S1B) solvent control and B[*a*]P treated mutants.

In the AHH-1 solvent control, a total of 14 spontaneous mutations were observed with deletions (93%) being the most dominant mutations (Figure 5A). The remaining 7% of mutations represented a single tandem mutation (TG285/6AT) (Supplementary Table S1A). B[*a*]P treated AHH-1 mutants showed predominantly (61%) point mutations, out of which 44.4% were G>T transversions. Other mutations such as C→T transitions (11%), insertions (5.5%), and deletions (33%) were also observed (Table I, Figure 5B). There were no transitions or transversions mutations in AHH-1 control cells and the ratio of transitions;transversions was 2:9 in B[*a*]P- treated cells. In the MCL-5 solvent mutants, 25 mutations were analysed and the mutational spectrum constituted 40% deletions, 36% transversions and 12% transitions mutations and 12% TG285/6AT tandem mutations (same mutation as AHH-1) were also observed (Table I, Figure 5C). B[*a*]P induced mutants predominantly contained point mutations (80%). Among all the point mutations, the proportion of G>T transversion mutations was higher (72% as compared to 4% transitions). The remaining 20% mutations detected were deletions (Table I, Figure 5D). The transitions:transversions ratio in control cells was 1:3 but for B[*a*]P-induced mutations it was 1:19. Most of the B[*a*]P induced mutations in AHH-1 and MCL-5 mutants were observed at exons 2 and 3 (Supplementary Table S1A and 1B). It was also noted that all G>T point mutations found in both MCL-5 and AHH-1 mutants were all on the non-transcribed strand. *CYP expression levels to explain cell lines specificity*

In order to explore if the expression levels of the key CYP450's explained the cellular differences observed in cytotoxicity/genotoxicity after B[*a*]P exposure, we studied mRNA expression of key CYP450's in

each cell line before and after B[*a*]P treatment. There was a difference in both the basal and induced expression of *CYP1A1*, *CYP1B1* and *CYP1A2* for all cell lines. Basal expression of *CYP1A1* in MCL-5, AHH-1 and HepG2 cells are shown in Figure 6. *CYP1B1* and *CYP1A2* were found only in MCL-5 and HepG2 (Figure 6b and c). Results from Real-time PCR showed an increase in expression of various CYPs with increasing concentrations of B[*a*]P, in both MCL-5 and HepG2 cell lines as compared to the untreated control. After 24h B[*a*]P treatment at the corresponding LOEL concentration, the induction of *CYP1A1* increased 29.2-fold ($p<0.001$) in MCL-5 and 16.81-fold ($p<0.01$) in HepG2 (Figure 6A). The change in *CYP1B1* expression, after 24h B[*a*]P exposure at the corresponding LOEL concentration was 10.52-fold ($p<0.05$) in MCL-5, but no effect was found in HepG2 (Figure 6B). B[*a*]P-induced *CYP1A2* expression was elevated by 4.43-fold ($p<0.001$) and 18.95-fold ($p<0.05$) in the MCL-5 and HepG2 cell lines respectively (Figure 6C).

3.5 CYP activity in different cell lines

CYP1A1, 1B1 and 1A2 enzyme activities in MCL-5, AHH-1, TK6 and HepG2 cultures were also assessed after 24h B[*a*]P exposure (Figure 7) using enzyme activity assays. CYP1A1 activity was significantly higher in MCL-5 than other cell lines, reflecting the mRNA results above. CYP1A1 activity increased significantly ($p<0.01$) with increase in concentration of B[*a*]P in all cell lines except TK6 (Figure 7A). CYP1B1 activity was significantly ($p<0.05$) high in both MCL-5 and HepG2 cells but was minimal in AHH-1 and TK6 (Figure 7B). *CYP1A2* activity was highly significant ($p<0.001$) in HepG2 cells at all treatments, reflecting the mRNA data above, with MCL-5 cells also showing activity. AHH-1 and TK6 cell did not show an increase in CYP1A2 activity at any treatment (Figure 7C).

4. Discussion

This study assessed the interplay between treatment and metabolic competence in determining genotoxic hazard *in vitro*. This is an important aspect in both hazard identification and risk assessment for chemicals that require metabolic activation. In the former, the most sensitive test is usually used to increase the

chances of detecting potential pro-mutagens, but in the latter, it is important to recognise the appropriateness of the system overall, to better reflect human risks.

4.1 Effect of differential metabolic competency on micronucleus frequencies after 4h and 24h exposure

The micronucleus assay data and gene expression and activity analysis of CYP1A1, CYP1B1 and CYP1A2 in the different cell lines showed a clear connection and positive correlation between CYP450 metabolic capacity and B[*a*]P's genotoxicity. Active AhR is the necessary requirement for the transcriptional activation of *CYP1A1*, *1A2* and *1B1* and thus conversion of B*a*]P into genotoxic metabolites. Indeed, *in vivo* studies by Shimizu *et al*. [38] have confirmed that upon B[*a*]P administration, tumour formation was only observed in AhR (+/+) and (+/-) mice but not in AhR (-/-) mice. Similarly, the more metabolically competent cell lines MCL-5 and HepG2, which express AhR, [39, 40] showed greater genotoxicity in response to lower concentrations of B[*a*]P than AHH-1 and TK6 cell lines. *CYP1A1* and *CYP1B1* mRNA expression levels and CYP450 activity in B[*a*]P treated cells was substantially higher in MCL-5 cells and this correlated with the highest frequency of B[*a*]P induced micronuclei. Similarly, cells with lower basal or induced expression of *CYP1A1* or other P450 enzymes showed little (AHH-1 cells) or no (TK6 cells) cytotoxic or genotoxic effect of B[*a*]P. Johnson *et al*. [41] also observed higher micronucleus frequencies in MCL-5 cells as compared to AHH-1 cell line for Azo dyes (Sudan 1 and Para red) which require metabolic activation. In the HepG2 cell line, an increase in B[*a*]P dose, resulted in a higher MN/BN frequency and an increase in CYP1A2 activity and expression, thus highlighting the role of CYP1A2 in B[*a*]P induced genotoxicity. Further, the treatment at which a significant increase in genotoxicity was first observed was much lower in MCL-5 and HepG2 cells than AHH-1 (Figure 1). The results obtained with AHH-1 cells support the earlier studies of Penman *et al*. [20] who also observed that lower levels of CYP1A1 and an absence of m*EH* made the AHH-1 cell line less metabolicaly competent. The link between m*EH* and B[*a*]P metabolism was observed when MCL-5 cells treated with NCND (an effective inhibitor for m*EH*) [37]. These findings indicate that B[*a*]P conversion to its mutagenic intermediates in cells devoid of m*EH* and with lower CYP1A1 levels, is slow and thus requires more time to convert similar quantities of B[*a*]P into its genotoxic metabolites .

Dose response thresholds for genotoxins can be used to assist the prediction of a safe exposure level. The theory behind genotoxic thresholds suggests that a compound will not produce an observable increase in DNA mutation below a critical exposure level and therefore, this does not increase the risk for the induction of cancer or congenital abnormalities. In this study, presence of a linear dose-response for MN at 24h exposure to B[*a*]P for all the metabolically competent cell lines may be explained by the potent formation of stable DNA adducts at N2-guanosine residues [42] which if left unrepaired, can block replication and transcription. Even a single BPDE-DNA adduct can effectively block expression of a reporter gene [43] and has been linked to mutations in multiple oncogenes including *p53* and *Kras*, causing severe damage to cell integrity, function and replication [44]. It is important to note however, that this linearity is intrinsically linked to metabolic capacity. It would be interesting to further study the dose responses to B[*a*]P in target tissues (e.g. lung) with intrinsic levels of metabolism likely to be far less than the MCL-5 and HepG2 cells here.

4.2 Comparison of the chromosome damage LOEL to the mutational LOEL

MCL-5 cells were more sensitive than AHH-1 cells to B[*a*]P-induced genotoxicity in general, which was likely due to the higher CYP450 enzyme expression in MCL-5 (Figure 6). However, the lesions that cause gene mutations (HPRT here) may be different from those that cause chromosomal breaks (micronuclei). Micronucleus formation occurs after multiple events including strand breaks during mitotic or failed DNA repair, whereas the HPRT assay can detect a single modification in the DNA mis-replicated during DNA synthesis. This increased assay sensitivity is reflected in the LOELs for HPRT mutations tending to be lower than those of MN induction. The LOELs in the CBMN assay after 24h B[*a*]P exposure were 3μM and 4μM in MCL-5 and AHH-1 cell lines respectively, whereas in the HPRT assay it shifted to 2μM in the MCL-5 cell line and remain unchanged in AHH-1. In the case of 4h B[*a*]P exposure, the LOEL was 40μM in CBMN assay and was 10μM in HPRT assay for MCL-5 cells.

4.3 Mutation spectra

HPRT mRNA was extracted and used to establish the spontaneous and induced mutation patterns in AHH-1 and MCL-5 cell lines. The B[*a*]P induced G to T mutations were all found on the non-transcribed

strand thus suggesting efficient transcription coupled repair of B[*a*]P DNA adducts on the transcribed strand. Mutation spectra of solvent control for both cell lines, AHH-1 (Figure 5A) and MCL-5 (Figure 5C) mainly consist of deletions whereas B[*a*]P treated cell lines mutation spectra shows a range of mutations (Figures 5B and D), mostly involving G to T transversions (implicating N2-dG adduct) supporting earlier reports where frequent G to T transversions were observed in the smoking associated mutational spectra of human lung cancer [45, 46]. Pfiefer *et al*. [46] also reported a high incidence of G to T transversions in *p*53 in lung samples as compared to larynx and the oral cavity of smoking associated cancers. Indeed, PAHs (such as B[*a*]P) present in smoke are believed to be responsible for the link between smoking and lung cancer. B[*a*]P from cigarette smoke has been linked with lung cancer, and studies [45] have reported distribution of BPDE adducts along exons of the *TP53* gene in BPDE-treated HeLa cells and bronchial epithelial cells. This study further showed adduct formation at guanine positions in codons 157, 248, and 273, which are believed to be major mutational hotspots in human lung cancer.

The strengths of this study include the comparison of cytotoxicity/genotoxicity in four cell lines coupling two genotoxic endpoints to the expression levels and activity of key CYP450's. The study evidences crucial links between metabolic activity, exposure time and genotoxic hazard posed by B[*a*]P. Weaknesses of the study include the use of secondary endpoints (cytotoxicity/genotoxicity) to infer metabolic activation of B[*a*]P as opposed to DNA adduct measurements and also the sole focus on phase I metabolism activating B[*a*]P without consideration for phase II detoxification.

In conclusion, this study shows that TK6 cells have negligible metabolic ability to metabolise B[*a*]P, and showed no cyotoxicity nor genotoxicity, confirming that B[*a*]P is non-toxic without metabolic conversion. We further show that CYP450 enzymes and m*EH* play an important role in the metabolic activation of B[*a*]P and the combined presence of CYP1A1, CYP1A2 and m*EH* caused MCL-5 and HepG2 cells to acquire more micronuclei and HPRT mutations compared to AHH-1 cells. The present study, thus emphasises the importance of considering the metabolic efficiency of *in vitro* cell systems when assessing dose responses to pro-carcinogens. We also suggest that metabolically competent cell lines offer an attractive alternative to rat liver S9 which may not necessarily be reflective of human liver physiology.

Conflicts of interest

Acknowledgements

This project was funded by Unilever (grant numbers CH-2009-1106).

References

1. Jackson, A.L. and L.A. Loeb. (2001). The contribution of endogenous sources of DNA damage to themultiple mutations in cancer. *Mutat Res,* 477(1-2), 7-21.
2. Waldron, H.A. (1983). A brief history of scrotal cancer. *Br J Ind Med,* 40(4), 390-401.
3. Yamagiwa, K., Ichikawa, K. (1918). Experimental study of the pathogenesis of carcinoma. *J. Cancer Res.,* 31-29.
4. Kennaway, E.L. and I. Hieger. (1930). Carcinogenic Substances and Their Fluorescence Spectra. *Br Med J,* 1(3622), 1044-6.
5. Cook, J.W., Hewett, C.L., & Hiege, I. (1932). Coal tar constituents and cancer. *Nature,* 130926-8.
6. Mandal, P.K. (2005). Dioxin: a review of its environmental effects and its aryl hydrocarbon receptor biology. *J Comp Physiol B,* 175(4), 221-30.
7. (ATSDR), U.S.C.f.d.c.a.f.t.s.a.d.r. (1995). "Toxicological profile for polyaromatic hydrocarbons (PAHs)".
8. Sgency., U.S.E.P. (2005). "Suppiemental guidance for Assessing Cancer Susceptibility from Early-Life exposure to Carcinogens".
9. Botteri, E., S. Iodice, V. Bagnardi, S. Raimondi, A.B. Lowenfels, and P. Maisonneuve. (2008). Smoking and colorectal cancer: a meta-analysis. *JAMA,* 300(23), 2765-78.
10. Neal, M.S., J. Zhu, and W.G. Foster. (2008). Quantification of benzo[a]pyrene and other PAHs in the serum and follicular fluid of smokers versus non-smokers. *Reprod Toxicol,* 25(1), 100-6.
11. Klareskog, L., L. Padyukov, and L. Alfredsson. (2007). Smoking as a trigger for inflammatory rheumatic diseases. *Curr Opin Rheumatol,* 19(1), 49-54.
12. Hattemer-Frey, H.A. and C.C. Travis. (1991). Benzo-a-pyrene: environmental partitioning and human exposure. *Toxicol Ind Health,* 7(3), 141-57.
13. Chepiga, T.A., M.J. Morton, P.A. Murphy, J.T. Avalos, B.R. Bombick, D.J. Doolittle, M.F. Borgerding, and J.E. Swauger. (2000). A comparison of the mainstream smoke chemistry and mutagenicity of a representative sample of the US cigarette market with two Kentucky reference cigarettes (K1R4F and K1R5F). *Food Chem Toxicol,* 38(10), 949-62.
14. Hoffmann, D., M.V. Djordjevic, and I. Hoffmann. (1997). The changing cigarette. *Prev Med,* 26(4), 427-34.
15. Scherer, G., S. Frank, K. Riedel, I. Meger-Kossien, and T. Renner. (2000). Biomonitoring of exposure to polycyclic aromatic hydrocarbons of nonoccupationally exposed persons. *Cancer Epidemiol Biomarkers Prev,* 9(4), 373-80.
16. Hanson-Painton, O., M.J. Griffin, and J. Tang. (1981). Evidence for cytosolic benzo(a)pyrene carrier proteins which function in cytochrome P450 oxidation in rat liver. *Biochem Biophys Res Commun,* 101(4), 1364-71.
17. Kim, D. and F.P. Guengerich. (2005). Cytochrome P450 activation of arylamines and heterocyclic amines. *Annu Rev Pharmacol Toxicol,* 4527-49.
18. Kirsch-Volders, M., L. Gonzalez, P. Carmichael, and D. Kirkland. (2009). Risk assessment of genotoxic mutagens with thresholds: a brief introduction. *Mutat Res,* 678(2), 72-5.
19. Jenkins, G.J., S.H. Doak, G.E. Johnson, E. Quick, E.M. Waters, and J.M. Parry. (2005). Do dose response thresholds exist for genotoxic alkylating agents? *Mutagenesis,* 20(6), 389-98.
20. Penman, B.W., L. Chen, H.V. Gelboin, F.J. Gonzalez, and C.L. Crespi. (1994). Development of a human lymphoblastoid cell line constitutively expressing human CYP1A1 cDNA: substrate specificity with model substrates and promutagens. *Carcinogenesis,* 15(9), 1931-7.
21. Crespi, C.L., F.J. Gonzalez, D.T. Steimel, T.R. Turner, H.V. Gelboin, B.W. Penman, and R. Langenbach. (1991). A metabolically competent human cell line expressing five cDNAs encoding procarcinogen-activating enzymes: application to mutagenicity testing. *Chem Res Toxicol,* 4(5), 566-72.
22. Doak, S.H., K. Brusehafer, E. Dudley, E. Quick, G. Johnson, R.P. Newton, and G.J. Jenkins. (2008). No-observed effect levels are associated with up-regulation of MGMT following MMS exposure. *Mutat Res,* 648(1-2), 9-14.
23. Aden, D.P., Fogel, A., Plotkin, S., Damjanov, I., & Knowles, B. B. . (1979). Controlled synthesis of HBsAg in a differentiated human liver carcinoma-derived cell line. . *Nature,* 282615-616.

24. Knowles, B.B., C.C. Howe, and D.P. Aden. (1980). Human hepatocellular carcinoma cell lines secrete the major plasma proteins and hepatitis B surface antigen. *Science*, 209(4455), 497-9.
25. Knasmuller, S., et al. (1998). Use of metabolically competent human hepatoma cells for the detection of mutagens and antimutagens. *Mutat Res*, 402(1-2), 185-202.
26. OECD. (2010). Organization of economic cooperation and development. Guidelines for the Testing of Chemicals, 487. *In vitro* Mammalian Cell Micronucleus Assay.
27. OECD. (1997). Guidelines for the Testing of Chemicals, 476. *In vitro* Mammalian Cell Gene Mutation Assay.
28. Brusehafer, K., B.J. Rees, B.B. Manshian, A.T. Doherty, M.R. O'Donovan, S.H. Doak, and G.J. Jenkins. (2014). Chromosome breakage induced by the genotoxic agents mitomycin C and cytosine arabinoside is concentration and p53 dependent. *Toxicol Sci*, 140(1), 94-102.
29. Seager, A.L., et al. (2012). Pro-oxidant induced DNA damage in human lymphoblastoid cells: homeostatic mechanisms of genotoxic tolerance. *Toxicol Sci*, 128(2), 387-97.
30. Seager, A.L., et al. (2014). Recommendations, evaluation and validation of a semi-automated, fluorescent-based scoring protocol for micronucleus testing in human cells. *Mutagenesis*, 29(3), 155-64.
31. Doak, S.H., G.J. Jenkins, G.E. Johnson, E. Quick, E.M. Parry, and J.M. Parry. (2007). Mechanistic influences for mutation induction curves after exposure to DNA-reactive carcinogens. *Cancer Res*, 67(8), 3904-11.
32. Thomas, A.D., G.J. Jenkins, B. Kaina, O.G. Bodger, K.H. Tomaszowski, P.D. Lewis, S.H. Doak, and G.E. Johnson. (2013). Influence of DNA repair on nonlinear dose-responses for mutation. *Toxicol Sci*, 132(1), 87-95.
33. Morgan, C. and P.D. Lewis. (2006). iMARS--mutation analysis reporting software: an analysis of spontaneous cII mutation spectra. *Mutat Res*, 603(1), 15-26.
34. Lutz, W.K. and R.W. Lutz. (2009). Statistical model to estimate a threshold dose and its confidence limits for the analysis of sublinear dose-response relationships, exemplified for mutagenicity data. *Mutat Res*, 678(2), 118-22.
35. Crespi, C.L., R. Langenbach, and B.W. Penman. (1993). Human cell lines, derived from AHH-1 TK+/- human lymphoblasts, genetically engineered for expression of cytochromes P450. *Toxicology*, 82(1-3), 89-104.
36. Gonzalez, F.J., C.L. Crespi, and H.V. Gelboin. (1991). DNA-expressed human cytochrome P450s: a new age of molecular toxicology and human risk assessment. *Mutat Res*, 247(1), 113-27.
37. Davis, B.B., D.A. Thompson, L.L. Howard, C. Morisseau, B.D. Hammock, and R.H. Weiss. (2002). Inhibitors of soluble epoxide hydrolase attenuate vascular smooth muscle cell proliferation. *Proc Natl Acad Sci U S A*, 99(4), 2222-7.
38. Shimizu, Y., Y. Nakatsuru, M. Ichinose, Y. Takahashi, H. Kume, J. Mimura, Y. Fujii-Kuriyama, and T. Ishikawa. (2000). Benzo[a]pyrene carcinogenicity is lost in mice lacking the aryl hydrocarbon receptor. *Proc Natl Acad Sci U S A*, 97(2), 779-82.
39. Nebert, D.W., A. Puga, and V. Vasiliou. (1993). Role of the Ah receptor and the dioxin-inducible [Ah] gene battery in toxicity, cancer, and signal transduction. *Ann N Y Acad Sci*, 685624-40.
40. Masten, S.A. and K.T. Shiverick. (1996). Characterization of the aryl hydrocarbon receptor complex in human B lymphocytes: evidence for a distinct nuclear DNA-binding form. *Arch Biochem Biophys*, 336(2), 297-308.
41. Johnson, G.E., E.L. Quick, E.M. Parry, and J.M. Parry. (2010). Metabolic influences for mutation induction curves after exposure to Sudan-1 and para red. *Mutagenesis*, 25(4), 327-33.
42. Lin, C.H., X. Huang, A. Kolbanovskii, B.E. Hingerty, S. Amin, S. Broyde, N.E. Geacintov, and D.J. Patel. (2001). Molecular topology of polycyclic aromatic carcinogens determines DNA adduct conformation: a link to tumorigenic activity. *J Mol Biol*, 306(5), 1059-80.
43. Koch, K.S., R.G. Fletcher, M.P. Grond, A.I. Inyang, X.P. Lu, D.A. Brenner, and H.L. Leffert. (1993). Inactivation of plasmid reporter gene expression by one benzo(a)pyrene diol-epoxide DNA adduct in adult rat hepatocytes. *Cancer Res*, 53(10 Suppl), 2279-86.
44. Yoon, J.H., C.S. Lee, and G.P. Pfeifer. (2003). Simulated sunlight and benzo[a]pyrene diol epoxide induced mutagenesis in the human p53 gene evaluated by the yeast functional assay: lack of correspondence to tumor mutation spectra. *Carcinogenesis*, 24(1), 113-9.

45. Denissenko, M.F., A. Pao, M. Tang, and G.P. Pfeifer. (1996). Preferential formation of benzo[a]pyrene adducts at lung cancer mutational hotspots in P53. *Science*, 274(5286), 430-2.
46. Pfeifer, G.P., M.F. Denissenko, M. Olivier, N. Tretyakova, S.S. Hecht, and P. Hainaut. (2002). Tobacco smoke carcinogens, DNA damage and p53 mutations in smoking-associated cancers. *Oncogene*, 21(48), 7435-51.

Type of Mutations	AHH-1 solvent control	AHH-1 B[*a*]P treated	MCL-5 solvent control	MCL-5 B[*a*]P treated
Point mutations	0	11	12	20
Transitions C > T		 2 (11%)	 3 (12%)	 1 (4%)
Transversions G > C C > G G > T		 1 (5.5%) 8 (44.4)	 5 (20%) 2 (8%) 2 (8%)	 1 (4%) 18 (72%)
Tandem mutations	1 (7%)		3 (12%)	
Deletions	13 (93%)	6 (33%)	10 (40%)	5 (20%)
Insersions		1 (5.5%)		

TABLE I. Percentages and Types of Spontaneous and Benzo-a-pyrene (B[*a*]P)-induced mutations (10μM) dose at the *HPRT* locus in AHH-1 and MCL-5 mutants after 24h exposure. Letters stands for bases; C (cytosine), T (thymine), G (guanine).

Legands

Fig. 1. Data of 24h exposure: Cytotoxicity (Relative population doubling (RPD) (%)) and micronucleus frequency (%MN/BN, micronuclei/binuclei) induced by increasing concentrations of Benzo[*a*]pyrene (B[*a*]P) in TK6, AHH-1, MCL-5 and HepG2 cell lines. The Lutz model outcome for micronucleus data, if linear, is labelled as "Linear". Line graphs show RPD and bars show %MN/BN. *, ** and *** indicates statistically significant results ($p<0.05$, 0.01 and 0.001 respectively) compared with that of the control samples. All data points represents the mean of three replicates. Error bars are standard error (SE).

Fig. 2. Data of 4h exposure: Cytotoxicity (%RPD) and micronucleus frequency (%MN/BN) induced by increasing concentrations of B[*a*]P in AHH-1, MCL-5 and HepG2 cell lines. The Lutz model outcome for micronucleus data, if linear, is labelled as "Linear". Line graphs show RPD and bars show %MN/BN. *, ** and *** indicates statistically significant results ($p<0.05$, 0.01 and 0.001 respectively) compared with that of the control samples. All data points represents the mean of three replicates. Error bars are SE.

Fig. 3. Effect of NCND, epoxide hydrolase inhibitor, on Cytotoxicity (%RPD) and micronucleus frequency (%MN/BN) in MCL-5 cells after 24h exposure to 70µM B[*a*]P. All data points represents the mean of three replicates. Error bars are SE.

Fig. 4. Gene mutation frequency (*HPRT*, bars) and Cell viability (%RPD, lines) induced by B[*a*]P. Dose response relationships at the *HPRT* gene in response to B[*a*]P for 4h (A) and 24h (B). All data points represents the mean of three replicates. Error bars are SE.

Fig. 5. Distribution of spontaneous (A and C) and Benzo[*a*]pyrene-induced (B and D) mutations in the *HPRT* gene in AHH-1 and MCL-5 mutants. Each base and its number on the HPRT sequence are presented on the *x-axis*. The number of mutations is portrayed on the *y-axis*. Each base alteration is colour coded where the letter

X stands for the 4 bases; A (argenine), C (cytosine), G (guanine) or T (thymine) determined by the position on the sequence. Numbers in the rectangular boxes represent the hotspots on exons.

Fig. 6. Basal and induced expression of (A) *CYP1A1*, (B) *CYP1B1* and (C) *CYP1A2* genes in the 4 cell lines after 24h exposure to B[*a*]P. The numbers 1 and 2 refer to the NOEL and LOEL dose for each cell line (for MN induction). (0) Untreated control, MCL-5 (1) 3μM, (2) 4μM; AHH-1 (1) 4μM, (2) 5μM; TK6 (1) 5μM, (2) 10μM; HepG2 (1) 3μM, (2) 4μM. Levels of *CYP1A1*, *1B1* and *1A2* mRNA were assessed by quantitative real-time PCR (A, B and C). Values were normalized using housekeeping gene β-actin and represent the mean fold change from vehicle control levels at each point for each cell line. After reverse transcriptase PCR, the samples were run on acrylamide gel and silver stained. The bands represent the expressions of *CYP1A1* (a), *CYP1B1* (b) and *CYP1A2* (c) in cell lines at different doses.

Fig. 7. Basal and induced phase I CYP1A1 (A), CYP1B1 (B) and CYP1A2 (C) enzyme activities (expressed as relative luminescence units [RLU]/cell number per well) in different cell lines after 24h exposure to B[*a*]P. (0) Untreated control, MCL-5- (1) 3μM, (2) 4μM; AHH-1- (1) 4μM, (2) 5μM; TK6- (1) 5μM, (2) 10μM; HepG2- (1) 3μM, (2) 4μM. ** and *** indicates statistically significant results ($p<0.01$ and 0.001 respectively) compared with that of the control samples. All data points represents the mean of three replicates. Error bars are SE.

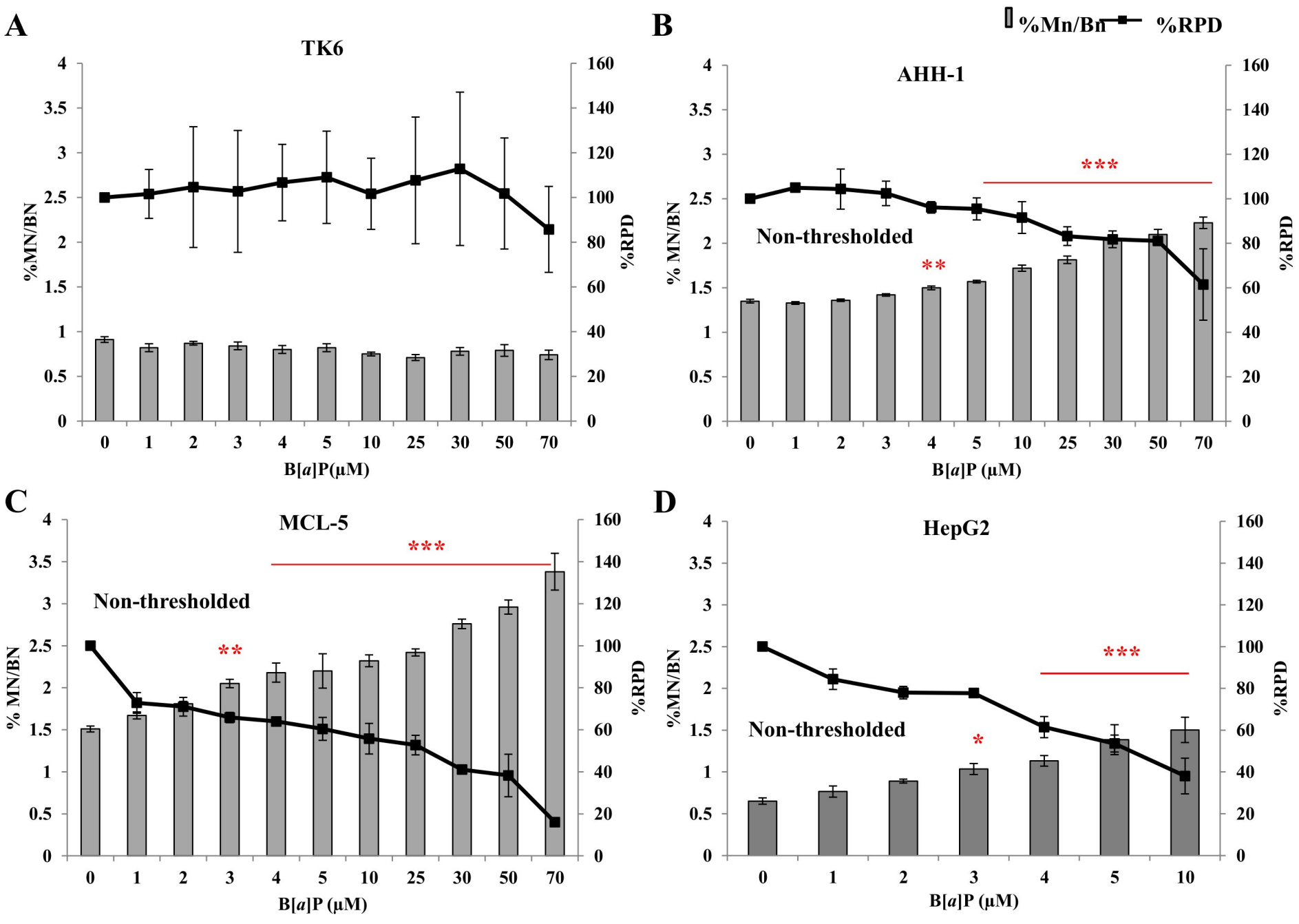
A
TK6
%MN/BN
%RPD
B[a]P(μM)
B
%Mn/Bn
%RPD
AHH-1
***
**
Non-thresholded
% MN/BN
%RPD
B[a]P (μM)
C
MCL-5
***
**
Non-thresholded
% MN/BN
%RPD
B[a]P (μM)
D
HepG2
***
*
Non-thresholded
%MN/BN
%RPD
B[a]P (μM)

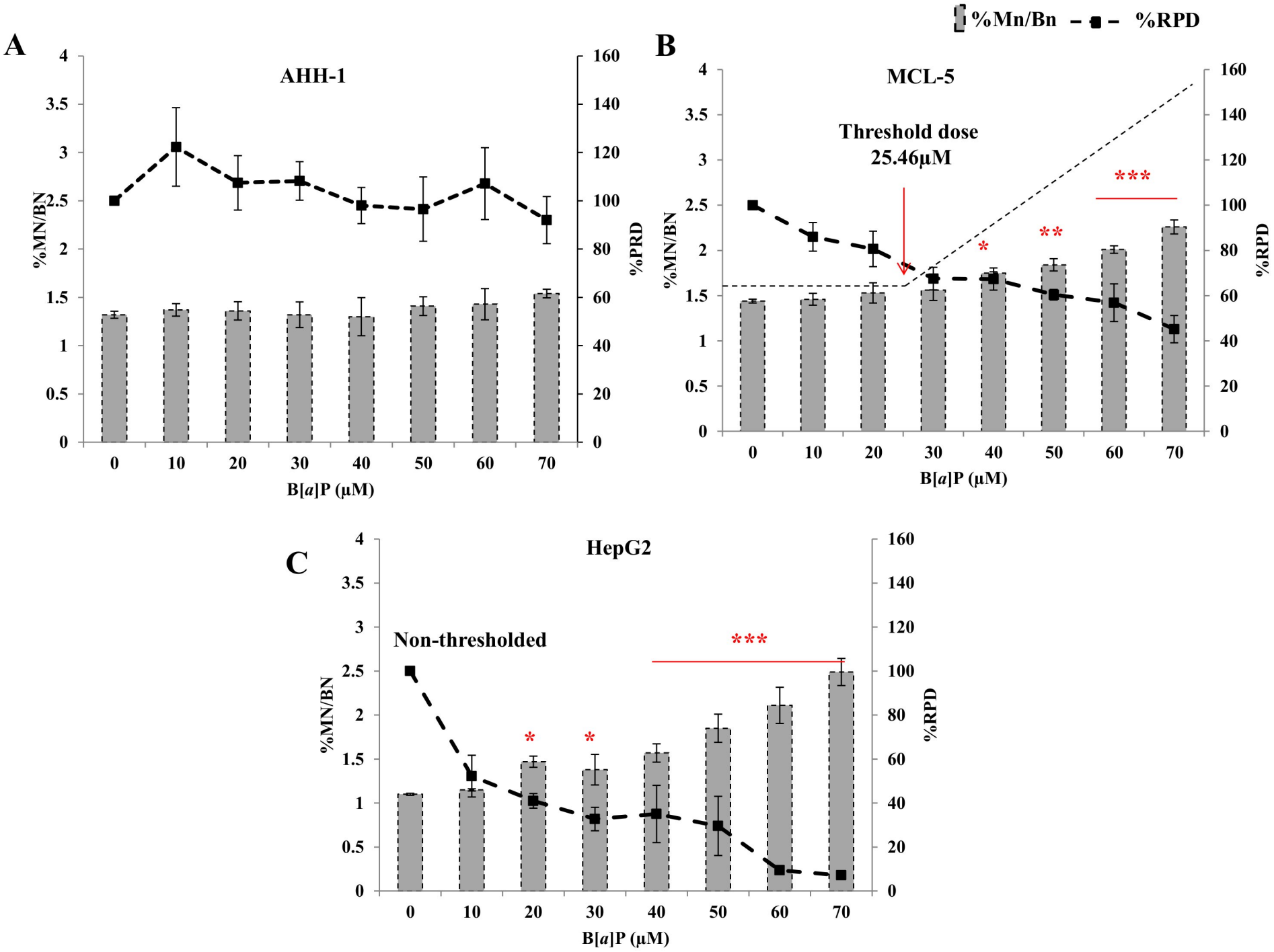
A
AHH-1
%MN/BN
%PRD
B[a]P (μM)
B
%Mn/Bn
%RPD
MCL-5
Threshold dose
25.46μM
***
*
**
%MN/BN
%RPD
B[a]P (μM)
C
HepG2
Non-thresholded
***
*
*
%MN/BN
%RPD
B[a]P (μM)

%MN/BN
%RPD
140
120
100
80
60
40
20
0
5
4.5
4
3.5
3
2.5
2
1.5
1
0.5
0
***
*
%RPD
%MN/BN
Control
NCND
B[a]P
NCND+B[a]P

A

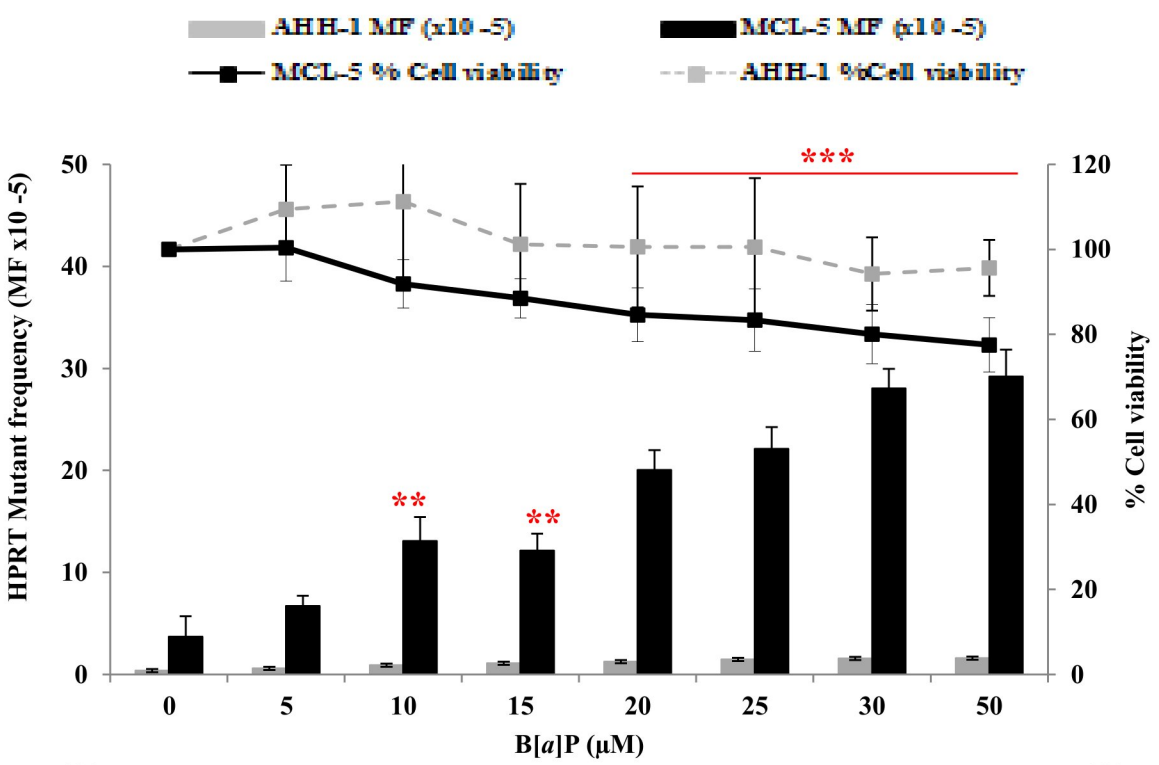
AHH-1 MF (x10 -5)
MCL-5 MF (x10 -5)
MCL-5 % Cell viability
AHH-1 %Cell viability
HPRT Mutant frequency (MF x10 -5)
% Cell viability
***
**
**
0
5
10
15
20
25
30
50
B[a]P (µM)

B

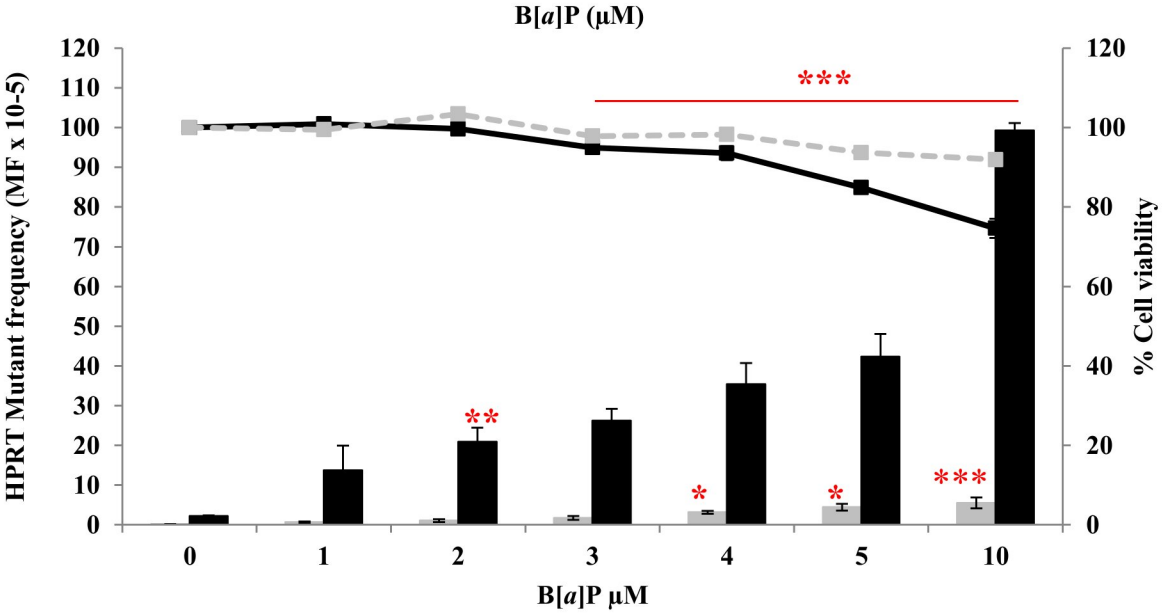
HPRT Mutant frequency (MF x 10-5)
% Cell viability
***
**
*
*
***
0
1
2
3
4
5
10
B[a]P µM

AHH-1 (A)

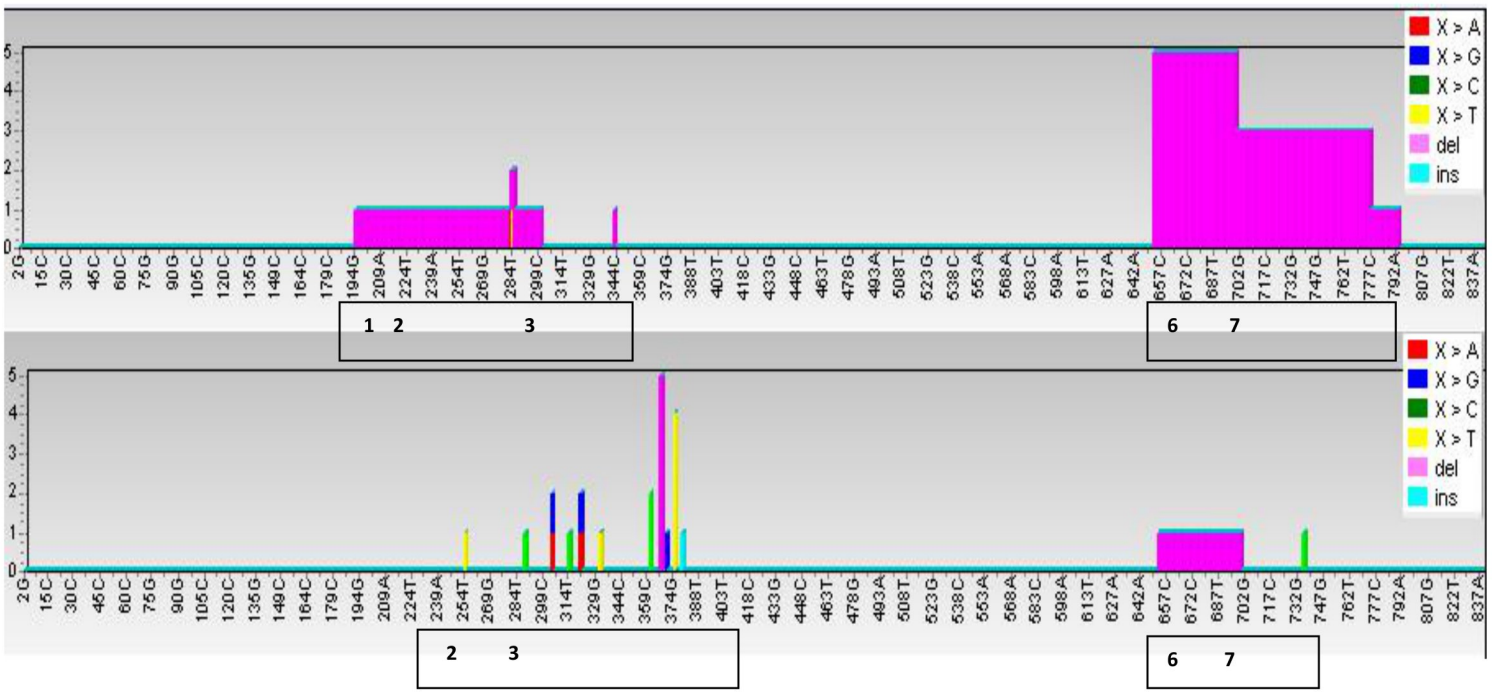

AHH-1 (B)

MCL-5 (C)

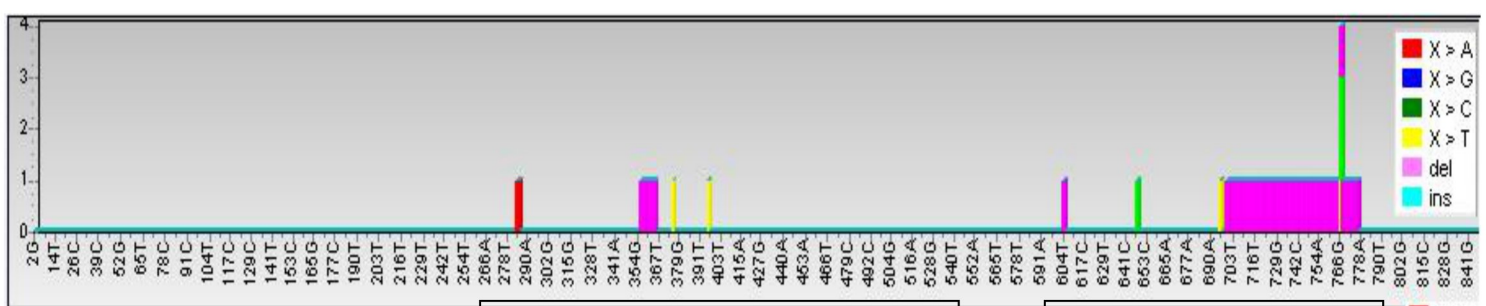

MCL-5 (D)

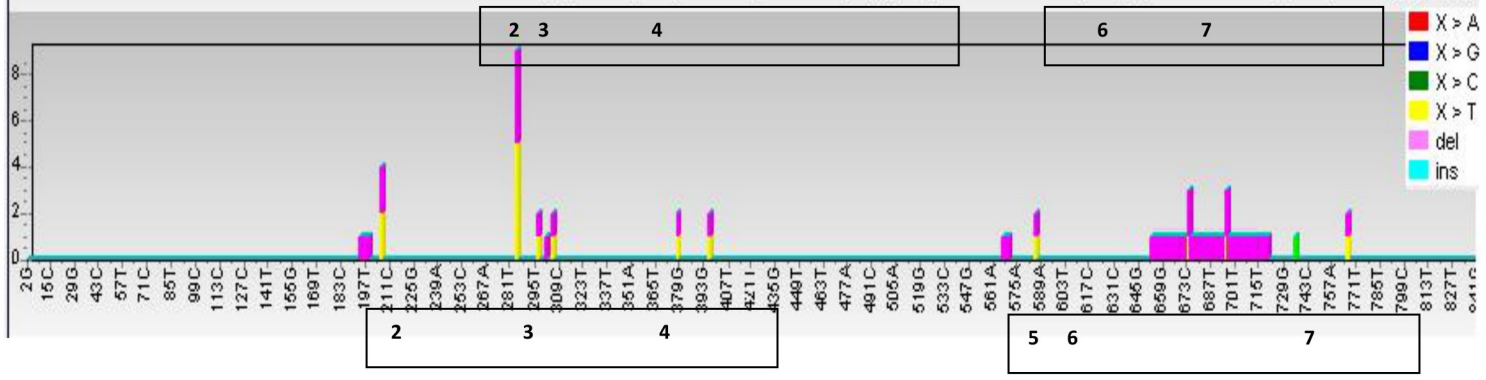

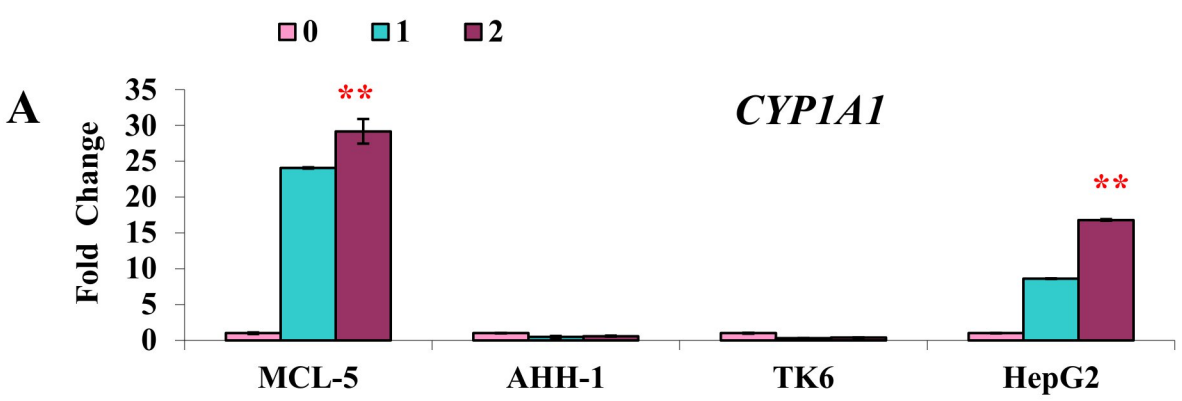
A
0
1
2
CYP1A1
Fold Change
35
30
25
20
15
10
5
0
**
**
MCL-5
AHH-1
TK6
HepG2

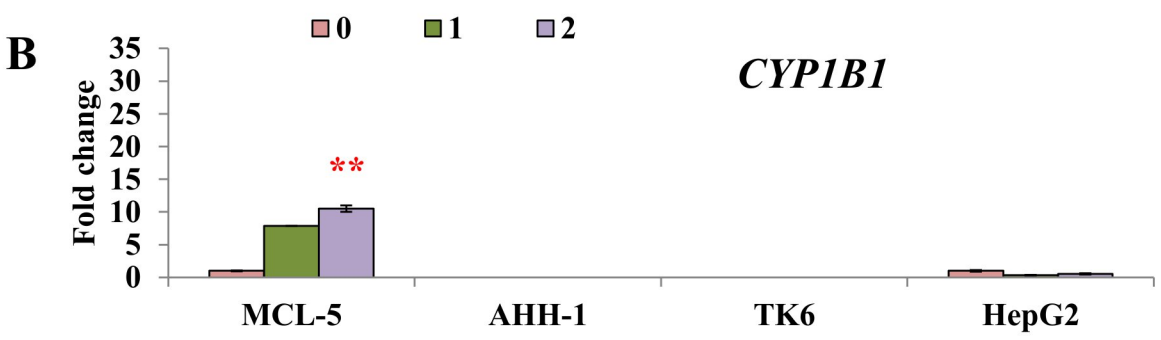
B
0
1
2
CYP1B1
Fold change
35
30
25
20
15
10
5
0
**
MCL-5
AHH-1
TK6
HepG2

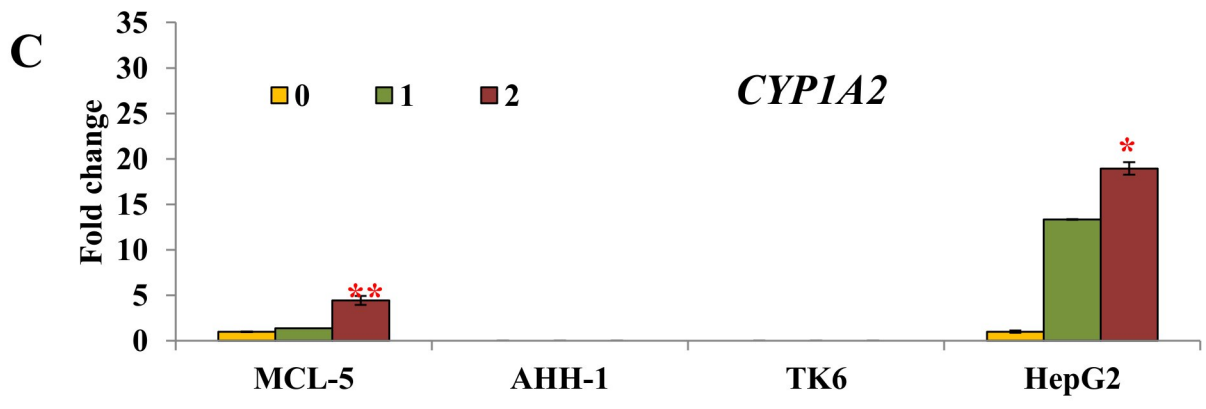
C
0
1
2
CYP1A2
Fold change
35
30
25
20
15
10
5
0
**
*
MCL-5
AHH-1
TK6
HepG2

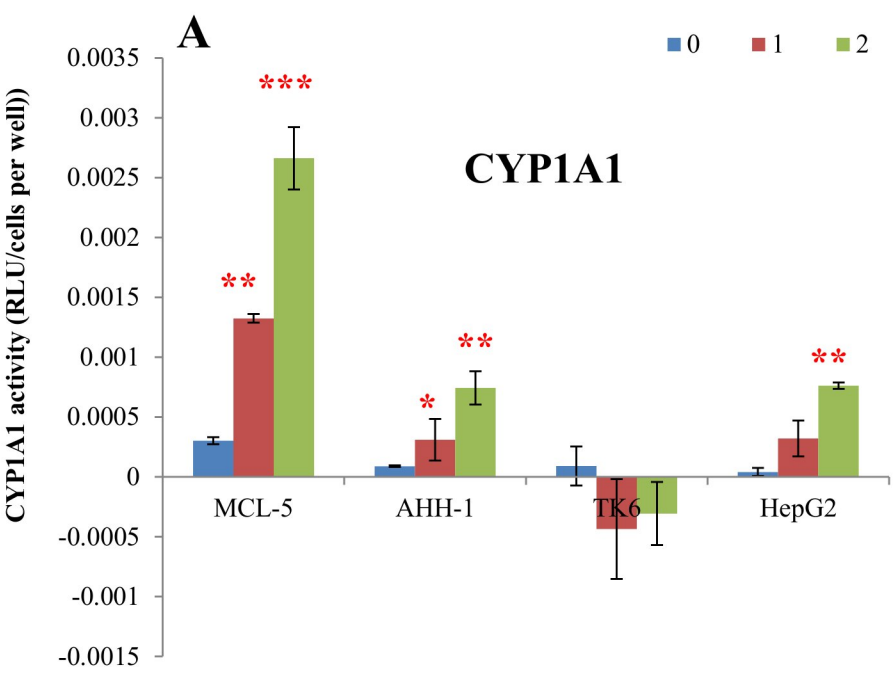
A
0
1
2
CYP1A1
CYP1A1 activity (RLU/cells per well))
0.0035
0.003
0.0025
0.002
0.0015
0.001
0.0005
0
-0.0005
-0.001
-0.0015
MCL-5
AHH-1
TK6
HepG2
***
**
*
**
**

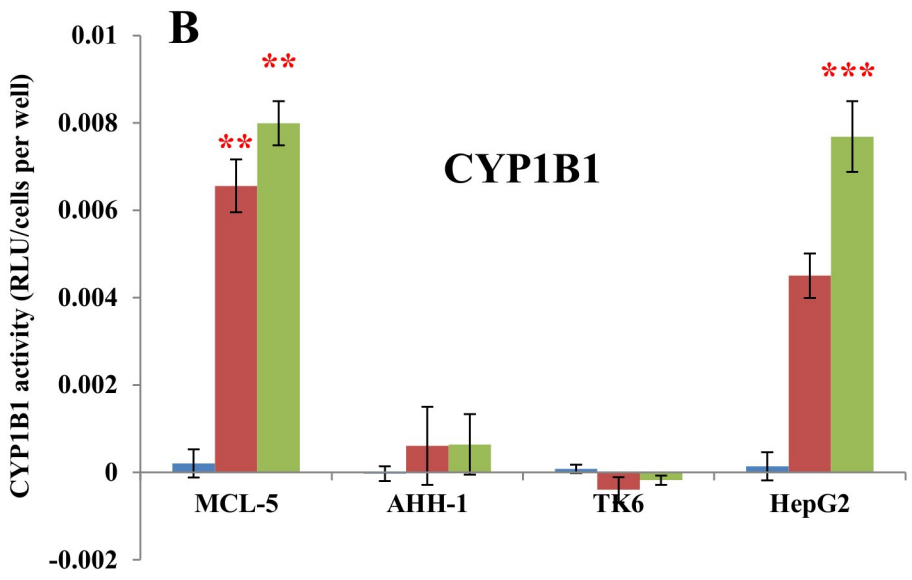
B
CYP1B1
CYP1B1 activity (RLU/cells per well)
0.01
0.008
0.006
0.004
0.002
0
-0.002
MCL-5
AHH-1
TK6
HepG2
**
**
***

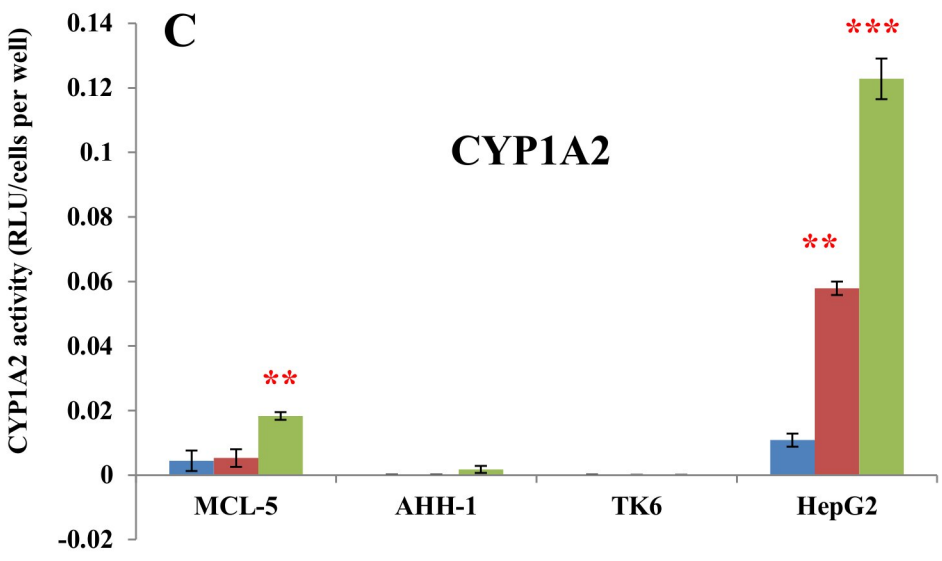
C
CYP1A2
CYP1A2 activity (RLU/cells per well)
0.14
0.12
0.1
0.08
0.06
0.04
0.02
0
-0.02
MCL-5
AHH-1
TK6
HepG2
**
**
***